Electronic Supplementary Material (ESI) for Nanoscale.

Supplementary Information

The Design and Synthesis of Spinel One-dimensional Multi-shelled Nanostructures for Li-ion Batteries

Hongli Li‡[a], Yantao Wang‡[b], Junwei Zhang*[a], Liu Zhu[a], Juan Shi[c], Bin Chen[a], Yang Hu[b], Hong Zhang[a], Xia Deng[a], and Yong Peng*[a]

[a] School of Materials and Energy, Electron Microscopy Centre of Lanzhou University and Key Laboratory of Magnetism and Magnetic Materials of the Ministry of Education, Lanzhou University, Lanzhou 730000, PR China

[b] College of Chemistry and Chemical Engineering, Electron Microscopy Centre of Lanzhou University, Lanzhou University, Lanzhou 730000, PR China

[c] College of Physics, Sichuan University, Sichuan 610065, PR China

*Corresponding authors: zhangjunwei@lzu.edu.cn or pengy@lzu.edu.cn

‡These authors contributed equally to this work.

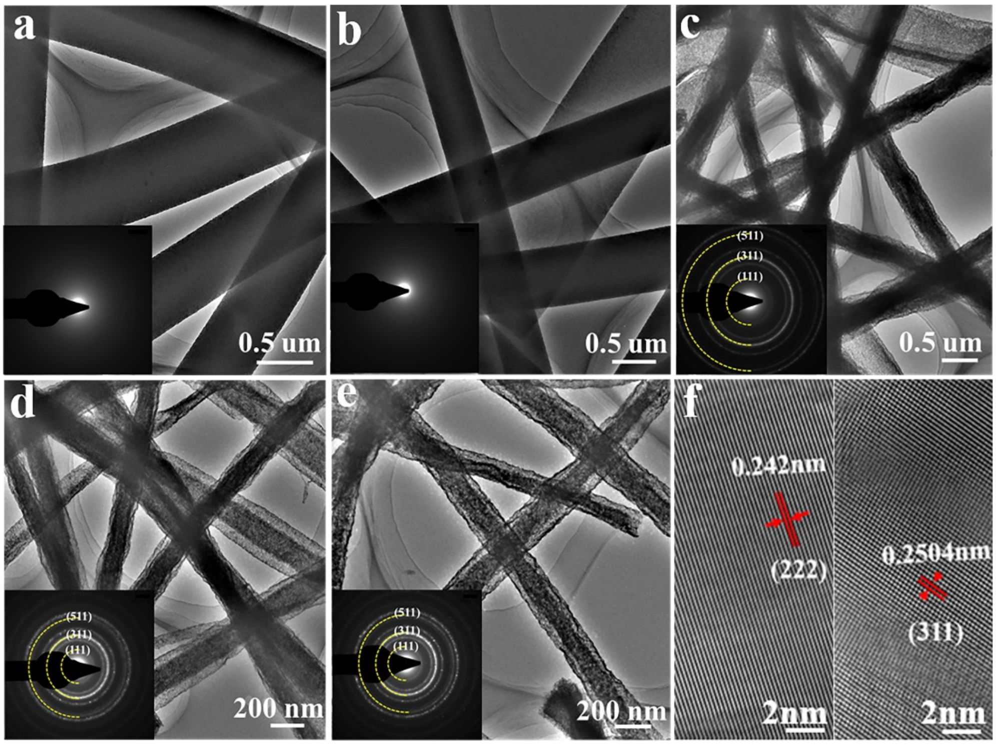

Figure S1. (a-e) TEM images showing the morphological evolution of $Co_{0.5}Ni_{0.5}Fe_2O_4$ tube-in-tube nanofibers during the calcination process at five temperatures and the insets is the SAED for the corresponding stages: (a) 200°C; (b) 250°C; (c) 300°C; (d) 400°C; (e) 500°C. (f) lattice fringe images corresponding to the nanoparticles made up of tube-in tube at 500°C in the TEM image.

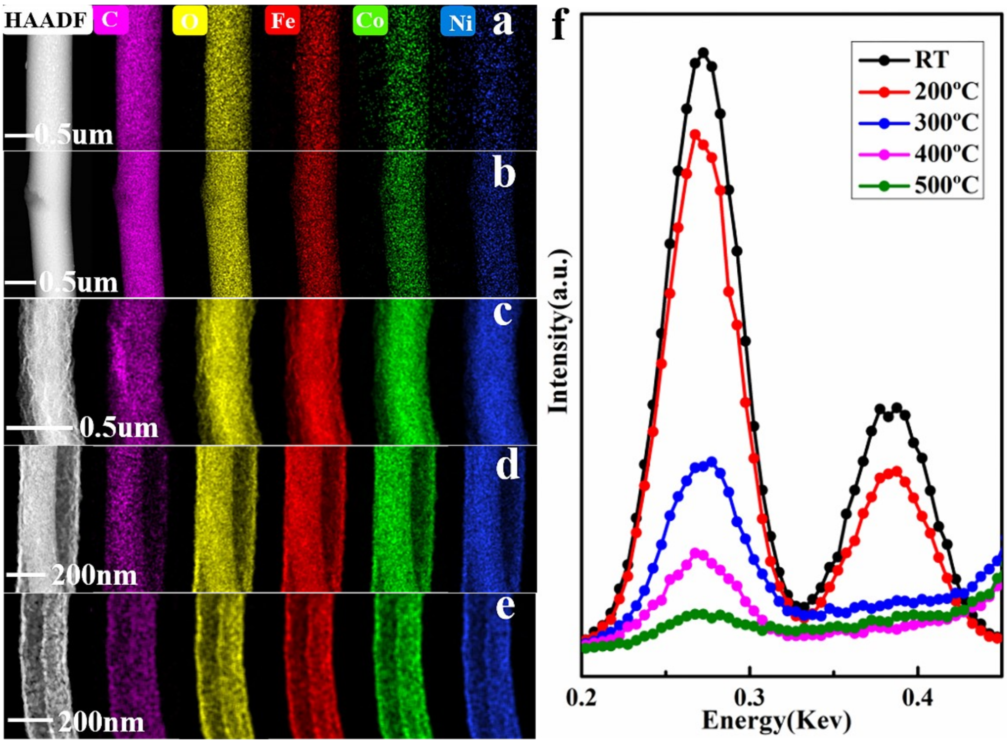

FigureS2. (a-e) STEM images of $Co_{0.5}Ni_{0.5}Fe_2O_4$ multi-shelled one-dimensional nanostructures at five temperature stages and the corresponding elemental mappings: (a) room temperature; (b)200°C; (c) 300°C; (d) 400°C; (e) 500°C. (f) Corresponding EDX spectra of carbon at different temperature stages.

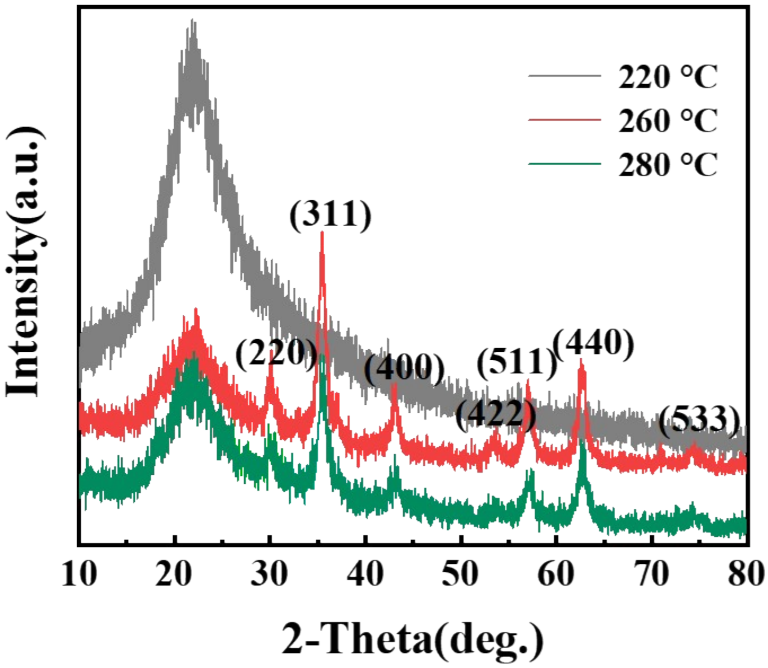

Figure S3. XRD spectra of Co0.5Ni0.5Fe2O4 tube-in-tube nanofibers calcined at three temperatures.

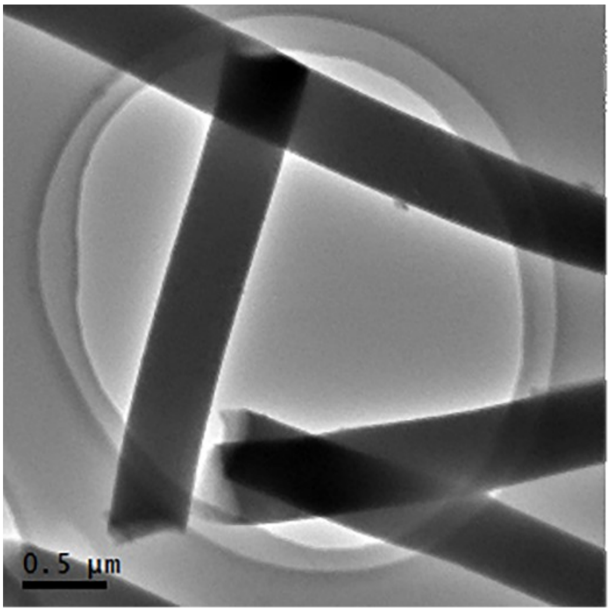

Figure S4. TEM images of $Co_{0.5}Ni_{0.5}Fe_2O_4$ nanorods which were obtained with 1g PAN in the precursor solution. The precursor nanofibers were heated to 500°C in N_2 atmosphere.

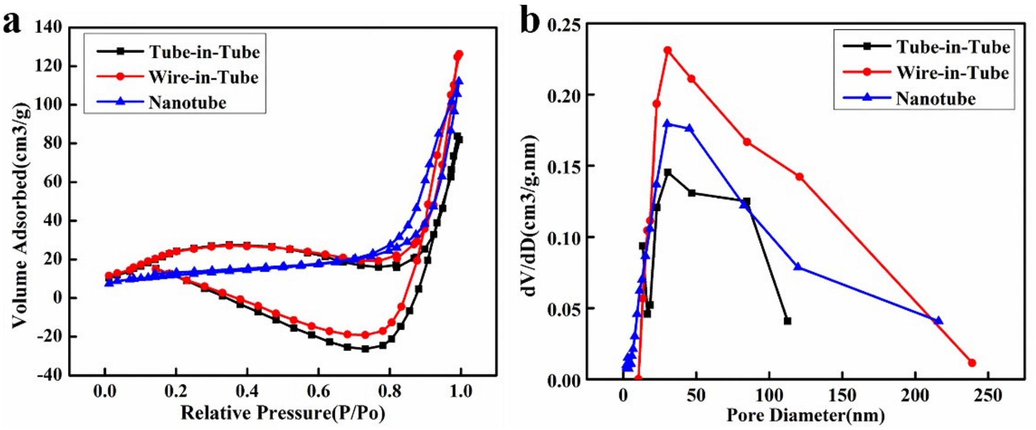

Figure S5. N2 adsorption/desorption isothermals of Co$_{0.5}$Ni$_{0.5}$Fe$_2$O$_4$ with different structures and the corresponding pore size distribution. The specific surface areas of Co$_{0.5}$Ni$_{0.5}$Fe$_2$O$_4$ tube-in-tube hollow structures are determined to be 94.9 m^{2}g^{-1} by Brunauer Emmett-Teller (BET) analysis compared to 90.9 m^{2}g^{-1} and 40.8 m^{2}g^{-1} for the Co$_{0.5}$Ni$_{0.5}$Fe$_2$O$_4$ wire-in-tube and nanotube structures, respectively. In addition, there is a wide pore size distribution for the Co$_{0.5}$Ni$_{0.5}$Fe$_2$O$_4$ samples verifying the porous structure.

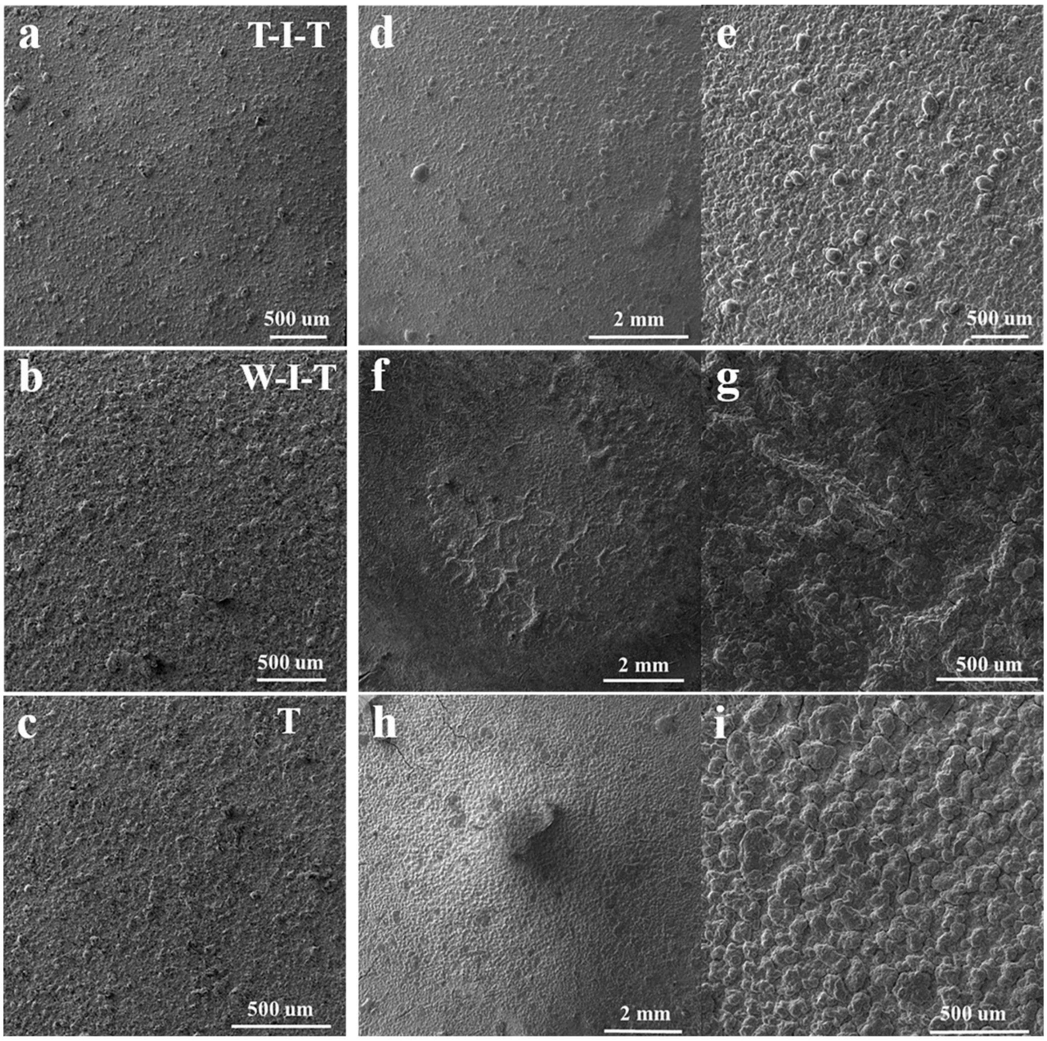

Figure S6. (a-b) SEM images before cycling for the electrodes of tube-in-tube nanofibers, wire-in-tube nanofibers, and single-shell nanofibers, respectively. (d-e, f-g and h-i) SEM images after cycling for electrodes of tube-in-tube nanofibers, wire-in-tube nanofibers, and single-shell nanofibers, respectively.

Figure S6 shows the SEM images of three kinds of nanofibers as electrodes before and after cycling. Comparing the surface structure of the electrode before and after the cycle, it is found that the surface of the electrode with tube-in-tube nanostructure is still smooth and uniform after the cycle, indicating that the electrode materials with tube-in-tube structure have good structural stability, thus achieving a better rate performance. For single-shell nanostructures, although the electrode surface is smooth after cycling, the surface cracks appear at the same time. At this time, the electrode material is easy to fall off from the collector, which indicates that the structure stability of the material is poor, and thus the rate performance is relatively poor. Therefore, the advantages of the tube-in-tube structure in rate performance can be obtained by comparing the structure of the electrode surface after cycling.

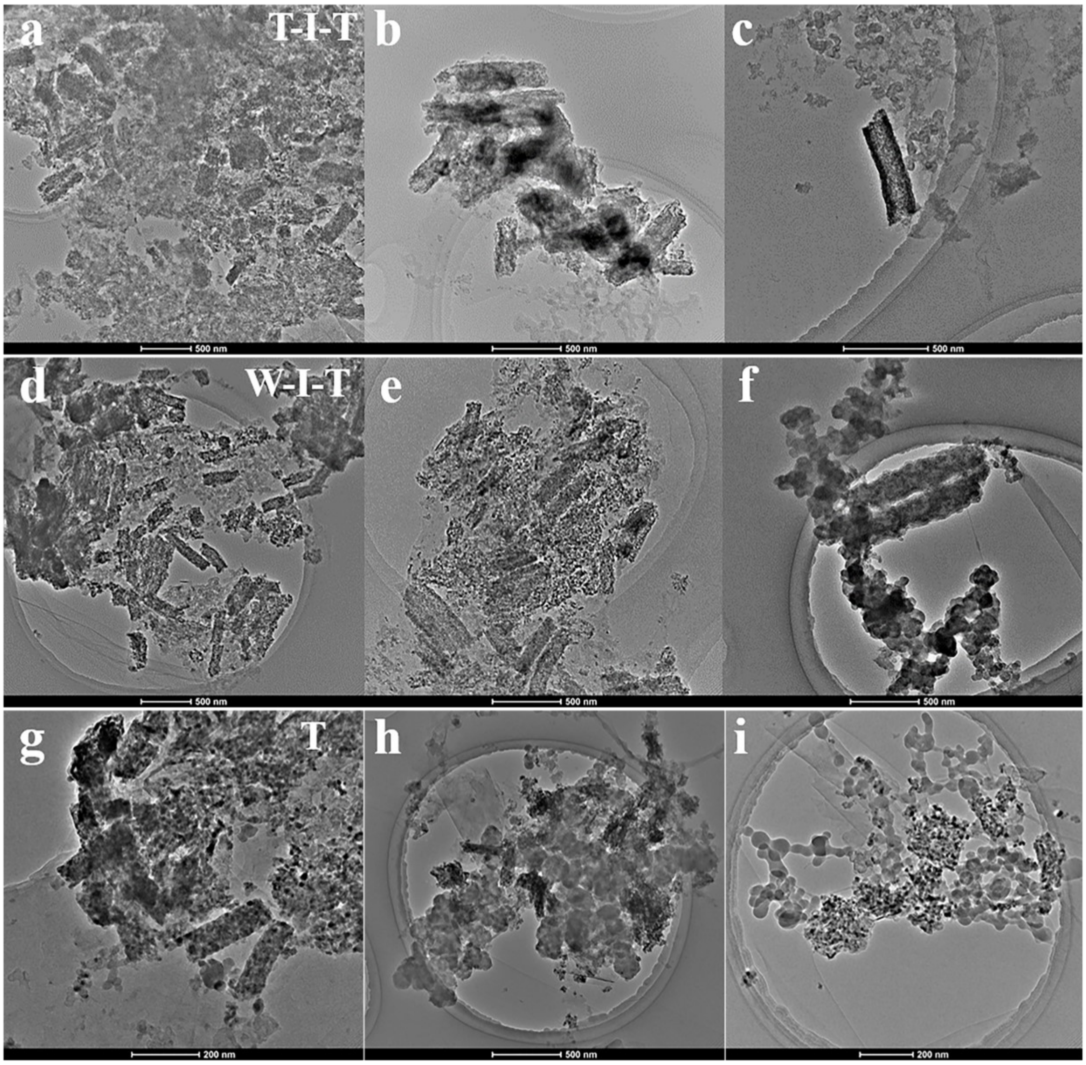

Figure S7 TEM images of morphological changes after cycling for electrodes of tube-in-tube nanofibers (a-c), wire-in-tube nanofibers (d-f), and single-shell nanofibers (g-i), respectively.

The TEM images show the morphological changes of three kinds of nanofibers as electrodes after cycling. It can be found that the structures of the tube-in-tube were still maintained the complete tube nanostructures, whilst the wire-in-tube and the single-shell nanostructures appeared partial fractures and collapses, among which the single-shell tube structure was the worst. Therefore, it is concluded that the tube-in-tube nanostructure can effectively improve the volume expansion of transition metal oxides during the cycle and severe structural changes caused by the rapid decay of the battery capacity.

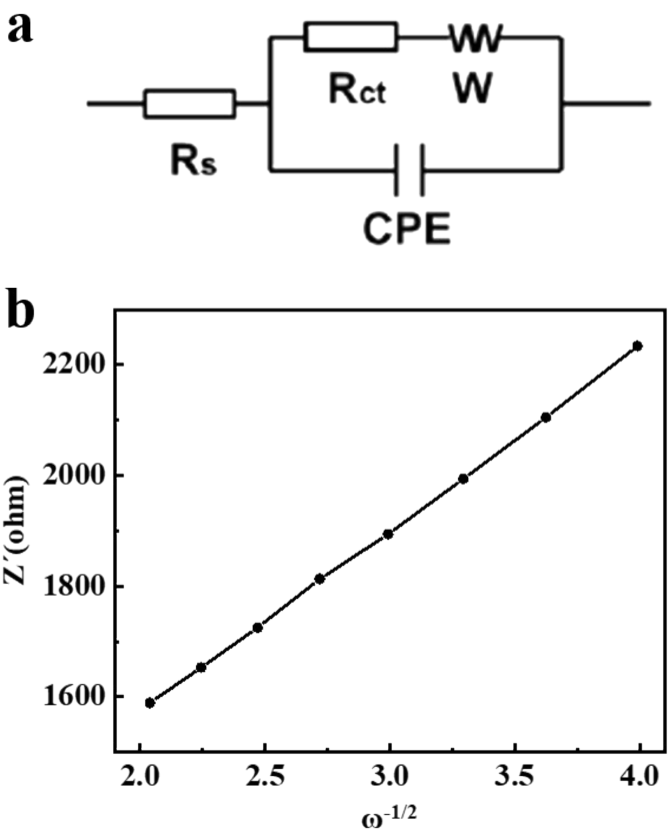

Figure S8. (a) The equivalent circuit model of EIS spectra. (d) plot of Z' versus $\omega^{1/2}$ in the low frequency region after three cycles.

Table 1. Summary of the EIS simulation results of the tube-in-tube $Co_{0.5}Ni_{0.5}Fe_2O_4$

nanofiber.

Cycle number	R_s (Ω cm^2)	R_{ct} (Ω cm^2)
1st cycle	5.197	434.6
2nd cycle	6.308	415.2
3rd cycle	6..294	410.9

The equivalent circuit model (Figure S8) corresponding to EIS data are drawn to fit the impedance spectra. The fitted parameter values of ohmic impedance (R_s) and charge-transfer impedance (R_{ct}) are shown in Table 1. As the number of cycles increases, charge-transfer resistance (R_{ct}) decreases and basically stabilizes. Furthermore, the Li^+ diffusion coefficient (D_{Li+}) can also be calculated from the following equation[1]:

$$D_{Li+} = \frac{R^2T^2}{2A^2n^4F^4C^2\sigma^2} \qquad (1)$$

where R is the gas constant (8.314 J/(mol·K)), T is the room temperature in the experiment (298 K), A is the surface area of the electrode, n is the number of electrons transferred in the reaction, F is the Faraday constant (96500 C/mol), and C is the concentration of lithium ions. σ is the slope of the $Z' \sim \omega^{-1/2}$ plot in figure b. The D_{Li+} value of the tube-in-tube $Co_{0.5}Ni_{0.5}Fe_2O_4$ nanofiber electrode after 3 cycles was calculated using equation (1), and the results is 2.3×10^{-14} cm^2 s^{-1}.

References

1. D. D. Wang, Z. Q. Shan, J. H. Tian and Z. Chen, *Nanoscale*, 2019, **11**, 520-531.